
Article:
Wright, D. and Ball, E. orcid.org/0000-0002-6283-5949 (2020) Highly portable, low cost SDR instrument for RF propagation studies. IEEE Transactions on Instrumentation and Measurement, 69 (8). pp. 5446-5457. ISSN 0018-9456

https://doi.org/10.1109/TIM.2019.2959422

Highly Portable, Low Cost SDR Instrument for RF Propagation Studies

D. P. Wright and E. A. Ball, *Member, IEEE*

***Abstract*—Software Defined Radio (SDR) instruments can be used to replace bulky and expensive spectrum analyzers for RF field measurements. Using commercial off the shelf (COTS) equipment a low cost, portable SDR instrument for measuring RF propagation has been created and tested. In the UK, parts of the VHF spectrum have been re-purposed for the use of Internet of Things devices, the instrument developed here is designed to meet the use-case of performing an urban propagation study in VHF and UHF Short Range Devices bands in a fast and low cost manner. Design of the hardware and software is discussed, as well as the calibration of the instrument. Results of a test propagation study are given for the completed instrument. It is shown that the SDR instrument is capable of performing the study to a high degree of agreement with a commercial spectrum analyzer, thus validating the approach. Readings of received power taken by the instrument are shown to agree with readings taken at the same locations with a commercial spectrum analyzer to within an average of 1.4dB at 71MHz and 1.1dB at 869.525MHz. From the measurements taken log distance models were able to be produced with a path loss exponent of 2.44 and log normal shadowing standard deviation of 8.5dB at 71MHZ and a path loss exponent of 4.06 and log normal shadowing standard deviation of 8.8dB at 869.525MHz.**

***Index Terms*—IoT, SDR, VHF, UHF, Raspberry Pi, RTL-SDR, Propagation, Path Loss.**

I. Introduction

PROPAGATION studies are currently conducted using expensive equipment and requiring time consuming measurement campaigns to produce enough readings to create a robust model. Current advances in software defined radio (SDR) and low cost, portable, commercial off the shelf (COTS) computing will be shown to be able to produce a low cost instrument that is capable of conducting a propagation study which can provide many hundreds of measurements in a very short amount of time. The focus of the study will be to produce an instrument capable of conducting this propagation study to a similar standard as a commercial spectrum analyzer within a specific use case and for specific frequencies. This will be accomplished by finding cost and complexity savings by focusing only on IoT propagation at specific frequencies, rather than attempting to replicate the entirety of the functions of a commercial spectrum analyzer. It is accepted that outside of the stated use case the performance of the instrument described in this paper will not be comparable to a commercial spectrum analyzer.

Manuscript received ??, 2019; revised ??, 2019.

D.P. Wright and E.A. Ball are with The University of Sheffield, Department of Electronic and Electrical Engineering, Portobello Centre, Pitt Street, Sheffield, UK, S1 4ET. (e-mail: dwright3@sheffield.ac.uk; e.a.ball@sheffield.ac.uk).

The novelty and contribution of this work is:

1) Low cost of the instrument with comparable performance to a spectrum analyzer over the stated frequency bands and use case.
2) The highly portable nature of the instrument, allowing hundreds or even thousands of measurements to be taken in a much shorter time than a traditional manual spectrum analyzer based study.
3) Producing an instrument capable of taking measurements and producing models which closely match an IoT deployment i.e. a close to ground, on body, mobile RX and a building height TX with distances starting from less than 1km. Current widely used empirical models such as Hata only cover distances greater than 1km, frequencies from 150MHz to 1500MHz and TX deployed at a height of at least 30m.
4) Producing an instrument capable of taking measurements in this IoT deployment style of newly re-purposed IoT spectrum in the VHF (˜70MHz) band. This spectrum has not previously been considered for urban IoT.
5) Initial results obtained from the platform are presented for an urban field trial, leading to a measurement based propagation model.

This paper is an extension of a conference paper previously published by the authors [1].

A. Newly Released IoT Spectrum

Internet of Things (IoT) is a large and rapidly growing field of communication technology, The IoT market is predicted to rise from 2bn devices in 2006 to 200bn devices in 2020 [2]. The commercial IoT implementations Sigfox and LoRa currently operate in the 868MHz Short Range Devices (SRD) band [3][4]. The UK telecommunications regulator, OFCOM, has re-purposed parts of the VHF spectrum for IoT use. The bands 55-68MHz, 70.5-71.5MHz and 80.0-81.5MHz [5] are now available. This is intended by OFCOM to stimulate the market for long range IoT solutions within the UK, primarily focused on rural implementations. Interest has also been shown in the USA and Japan for re-purposed, now vacant, VHF and UHF television bands [6]. It is considered in this work that this new VHF spectrum could also be useful in the urban environment. In order to investigate these newly available bands and identify the characteristics of their use in an urban IoT use case, a propagation study should be conducted.

An SDR based instrument using COTS equipment will be created to allow an urban propagation study to be conducted quickly and cheaply, using both the re-purposed VHF and

currently used UHF bands at 868MHz. In future work the results collected at these two bands can then be compared to each other in order to assess their relative strengths and weakness within an urban IoT use-case. The instrument will be designed to be low cost, highly portable (to allow it to be carried discretely through an urban area) and capable of taking readings quickly in order to reduce the time taken to perform a study requiring many hundreds of readings.

B. Existing Published Approaches to Conducting Propagation Studies

A number of propagation studies were identified in order to assess the equipment used in such studies, those dealing with IoT uses or VHF were investigated most closely. No studies addressing all the key areas of VHF, urban area and IoT use cases were found.

Fuschini *et al.* [7] provides details of an indoor to outdoor propagation study at 169MHz for IoT smart metering. A HP 8663A signal generator is used to produce a 27dBm CW signal, transmitted via a Yagi antenna. RX readings are provided by a Narda SRM3000 portable spectrum analyzer connected to a helical antenna. Readings of received power were taken at multiple stationary positions around the perimeter and inside of the test building.

Faruk *et al.* [8] studies propagation at VHF and UHF with regards to urban clutter and changes in terrain. TX was provided via the utilization of the signals of local TV transmitters with known power (1kW to 7kW), position and frequency. RX readings of the received signal strength are provided by an Agilent N9342C portable spectrum analyzer connected to a omni-directional whip antenna capable of covering 70MHz to 1GHz, a GPS receiver was also connected to the spectrum analyzer to record measurement positions. The RX set up was driven along predefined routes with multiple measurements of received power taken.

Andrusenko *et al.* [9] studies ground-to-ground propagation over distances less than 1km at frequencies of 30MHz to 88MHz. The work focuses on indoor or indoor-to-outdoor propagation, only line of sight outdoor-to-outdoor scenarios are considered. The TX consists of a Wiltron 68177B signal generator producing a CW signal connected to a high power amplifier and a whip antenna. RX readings are provided by an HP 8562A connected to a bandpass filter, LNA and whip antenna. The RX set up was moved along predefined routes with multiple measurements of received power taken.

All the above identified studies involved the use of very expensive equipment, with some of the portable spectrum analyzers used costing up to $35,000 when new. Some of these analyzers can measure frequencies up to 22GHz, which is far in excess of the frequencies required. Cost and complexity savings could be made in the designed SDR instrument by reducing this frequency range to focus on the IoT frequencies of interest. Table I shows a comparison of the spectrum analyzers used in the listed studies as well as the one used in this study to validate the readings of the SDR instrument.

Certain requirements for a propagation study become evident from examining the identified studies. The studies only measure received signal intensity, usually of a CW signal, no multipath readings are taken for example to measure delay spread. Readings must be taken at a number of locations across a chosen area. So the designed instrument must be capable of recording a measurement of intensity and frequency of a signal along with the location the measurement is made at. The process should be automated as far as possible in order to reduce the time taken to perform a study.

TABLE I
COMPARISON OF THE COMMERCIAL SPECTRUM ANALYZERS USED IN THE IDENTIFIED STUDIES

Make	Model	Frequency Range	DANL (dBm/Hz)	Cost	Study
Narada	SRM3000	100KHz to 3GHz	-151	$15,500	Fuschini [7]
Agilent	N9342C	100Hz to 7GHz	-164	$12,249	Faruk [8]
HP	8562A	1KHz to 22GHz	-130	$35,000	Andrusenko [9]
Anritsu	MS2712E	9KHz to 4GHz	-162	$9,000	This Study

Delay spread has previously been measured in the test area, at the frequencies used in this paper, by one of the authors in [10]. Maximum RMS delay spread was found to be less than $1\mu s$. IoT systems have a low data rate, and therefore a low symbol rate, for example LoRa ranges from 0.3kbps to 50kbps [4]. This means the symbol duration is between 3.3ms and 20μs, because the symbol duration is much greater than the RMS delay spread the system will experience negligible levels of Inter-symbol Interference (ISI) [11].

In order to save time and money, cost and complexity savings will be made by focusing only on the frequencies and bandwidth of the IoT signals that are of interest. The spectrum analyzer used in the identified studies are able to operate up to multiple GHz and produce wide band measurements, but this holds no benefit when all the signals of interest are in the MHz range and have a narrow bandwidth. It is therefore evident that an instrument with this focus will lead to significant savings.

C. Software Defined Radio

Software Defined Radio (SDR) involves transferring the functions of a radio from a hardware focus to a software one. It consists of the minimum amount of hardware necessary to receive an RF signal and convert it to a digital signal that is readable by a processing device such as a computer, microprocessor or FPGA. Software DSP techniques are then used to manipulate the digital signal in to useful information, also making the radio easier to modify and update via software updates and eliminating the requirement for expensive and time consuming hardware revisions.

Software defined radio has previously been used to produce measurement instruments. Through their high-precision measurements of sine and pulse reference signals, Andrich *et al.* [12] have shown that it is possible for an SDR instrument to provide highly accurate readings, surpassing commercially available lab equipment.

Bilski *et al.* [13] produced a real time virtual spectrum analyser using software defined radio techniques within National Instruments (NI) LabVIEW environment and propitiatory NI hardware. However this system wasn't designed for portability

and still used expensive hardware. LabVIEW was also used by Schmidt *et al.* [14] and Soghoyan *et al.* [15] to create SDR GPS receivers which allow rapid prototyping of new GPS techniques. The general use of LabVIEW is now widely accepted in the automatic test equipment community, this shows the value of an SDR instrument and the willingness of the community to adopt them.

Yarkan [16] produced an SDR measurement set up to evaluate spectrum sensing techniques in indoor environments. This set up was created using an expensive R&S TSMQ radio network analyzer to receive and digitize RF signals in to IQ data which is fed in to laptop for processing. This set up therefore allows for the SDR benefit of re-programmability, but no cost benefit and poor portability.

Goverdovsky *et al.* [17] produced an SDR based test bed intended to test direction finding algorithms. Universal Software Radio Peripheral (USRP) boards from Ettus Research (part of NI) provided hardware. The test bed showcased the inherent re-programmability of an SDR based instrument with multiple different algorithms deployed. Using an SDR instrument, it is possible to rapidly develop, prototype and test new measurement techniques cheaply without requiring hardware changes.

SDR instruments have also been used to test ways of characterizing RFID tags [18] [19], locating non-cooperative superheterodyne radio receivers [20] and to evaluate algorithms for Blind Wireless sensing [21].

II. SDR Based Instrument

For our instrument both hardware and software will be considered. The instrument will consist of 3 parts: hardware; on-device processing software; and post processing software. Due to the license granted by OFCOM for this work the frequencies examined by the instrument will be 869.525MHz in the SRD band and 71MHz in the newly re-purposed band. However, due to the use of the RTL-SDR device the instrument could be used to investigate any number of frequencies from 25MHz to 1750MHz. While the RTL-SDR could support broadband readings by using the developed program to sweep the local oscillator, since IoT transmissions are regulated to bandwidths much smaller than the 2.048MHz bandwidth that it is possible to realize without sweeping, it was decided that broadband readings were unnecessary. The requirements for the instrument are as follows:

- Dual Band - The instrument must be able to record measurements at both 71MHz and 869.525MHz in quick succession in order for the two bands to be studied at near the same time and location. Assuming an average walking speed of 1.3m/s measurements should be taken within approximately 2s to keep the readings within 2.6m of each other.
- Portable - The instrument, including antennas, must be light and compact enough for a person to carry unaided, allowing the instrument to be carried through all pedestrian accessible parts of an urban test area, in the same way an IoT device might be carried.
- Low cost - As shown in table I the equipment for a propagation study is extremely expensive, this limits who can perform a study. Where possible COTS parts will be used in this instrument in order to reduce costs and make the system accessible to more people such as universities and small businesses.
- Automated - Once activated the instrument should require no action from the user to collect measurements, reducing complexity and therefore speeding up the process of conducting a propagation study. This includes the instrument detecting and recording its own location, via GPS, along with measurements.

Fig. 1. Picture of the SDR instrument as realized

Because of the automated and portable nature of the instrument it is envisioned that many hundreds of measurements can be made quickly across a large area, providing as much information as possible for analysis. Fig. 1 shows the assembled instrument.

A. Hardware

The key enabling technology for this work is the COTS RTL-SDR device produced by NooElec, which is based on a USB DVB-T television receiver for a PC. The device contains a Realtek RTL2832u demodulator which can convert received signals to an in-phase and quadrature (IQ) data format, it is this ability that allows this device to be used as part of a low cost SDR system. The RF front end of the device uses a Rafael Micro R820T2 RF tuner IC with a frequency range of 25MHz to 1750MHz. A Temperature Compensated Crystal Oscillator (TCXO) with a frequency stability of 0.5ppm is also included. The cost of this device is approximately £25 [22]. Drivers are available for the Linux and Windows operating systems, with MATLAB and Python supporting programming for the device. Fig.2 shows an overview of the architecture of the entire SDR instrument, including the internal functions of the RTL-SDR device.

A Raspberry Pi (RPi) model 3B is used as the processing and control device for the instrument. This COTS device features a 1.2GHz quad core 64-bit CPU and 1GB of RAM [23], allowing it to easily meet the expected computational requirements. The RTL-SDR device and other peripherals can be connected and controlled via the 4 USB ports. General Purpose Input and Output (GPIO) pins on the RPi can also be

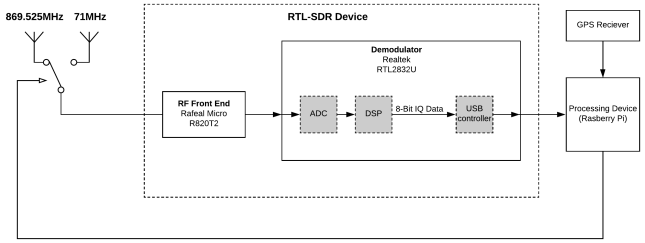

Fig. 2. Architecture of the SDR instrument including the internal arrangement of the NooElec RTL-SDR device

used to control other devices via user created programs. The RPi is small and lightweight with low power consumption requirements, making it ideal for use in a portable instrument. The RPi costs approximately £35.

The RPi requires a power source capable of providing up to 2.5A at 5V via USB, this power source will also power the RTL-SDR and GPS dongle via the RPi. In order to provide portable power a COTS mobile phone power bank type battery was selected at a cost of approximately £30.

In order to automate the collection of location data for the instrument when a measurement is taken, GPS functionality has been implemented via a COTS USB Dongle using a Ublox UBX-M8030 chipset connected to the RPi, costing approximately £20.

Because measurements of two bands are required and the design of a dual-band receiver (as shown by Liu [24]) is outside the scope of this work, in order to conduct measurements of both bands of interest in quick succession a switch between two antennas, with each antenna suited to a specific band, has been created. The GPIO connector on the RPi is used to control an RF switching circuit, with switching instructions issued automatically by the control software on the RPi. A sleeved dipole is used for 869.525MHz measurements and a helical antenna is used for 71MHz measurements in order to keep the antenna size appropriate for pedestrian usage.

The total cost of the COTS parts in the SDR based instrument is approximately £110, compared to $9,000 for the Anritsu MS2712E portable spectrum analyzer used to take comparison readings in this study.

B. On-System Measurement Algorithm

Data and initial measurements are collected in the field by the SDR instrument, with the results being saved for later post-processing into path loss information. The on-system measurement algorithm is implemented using the Python programming language. Fig. 3 shows the output of the algorithm at one frequency for one sampling period with the instrument fed from a signal generator emitting -95dBm at 869.525MHz. A large peak can be seen at the center of the figure, which has been detected at a frequency of 869.525MHz and the amplitude of this peak is recorded as -95.3dBm. A smaller peak can be seen to the right of the large peak, this is produced by DC leakage from the RTL-SDR and is ignored by the algorithm.

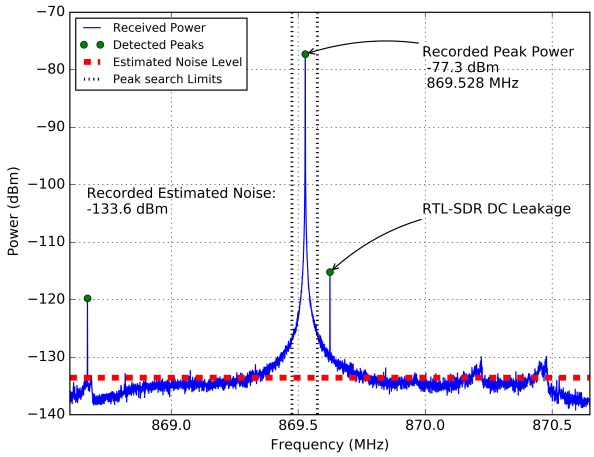

Fig. 3. An annotated example of an RF signal (produced by a signal generator) received during one sampling period by the SDR instrument.

The algorithm can be thought of in two stages, 1) data is collected and then 2) initial measurements are made of noise and detected peak frequencies and amplitudes.

Fig. 4 shows the method of the data collection stage for one frequency. The algorithm first controls the antenna switch via the GPIO outputs of the RPi, selecting the appropriate antenna for the current measurement.

GPS co-ordinates for the instrument's current position are taken in decimal degrees and saved to a comma separated values (.csv) file for later post processing.

RTL-SDR device is set up with the following parameters: the device is tuned to the center frequency of the channel that is currently being measured, this observation frequency (Fch) is either 71MHZ or 869.525MHz in this work. A sampling frequency of 2.048MHz was chosen for the RTL-SDR device because this is the highest available rate that guarantees the stability of the driver and no lost samples. The algorithm collects 5000 samples to give a resolution bandwidth (RBW) of 409.6Hz. A total of 5000 samples can be collected in 2.44ms at this sampling frequency. Achieving the highest speed possible is important due to the mobile nature of the instrument, readings will be taken while the instrument is in motion, so the faster the collection is the more the measurements are localized to one position. A discussion of the the chosen RTL gain will be given in section II-D.

The algorithm performs a Fast Fourier Transform (FFT), sampling and FFT calculation is performed one hundred times, with the results averaged in order to provide a smoother and more readable spectrum with reduced noise. The resulting spectrum is represented by the solid blue line in Fig. 3. The time taken to collect data, produce the FFT and conduct averaging has been measured as 0.36s, 0.24s of this time can be attributed to the time it takes to record 5000 samples one hundred times. The averaged FFT is saved as a binary file for later examination, it is then passed on to the measurement part of the algorithm

Fig. 5 shows how initial measurements are taken from the averaged FFT produced in the data collection stage.

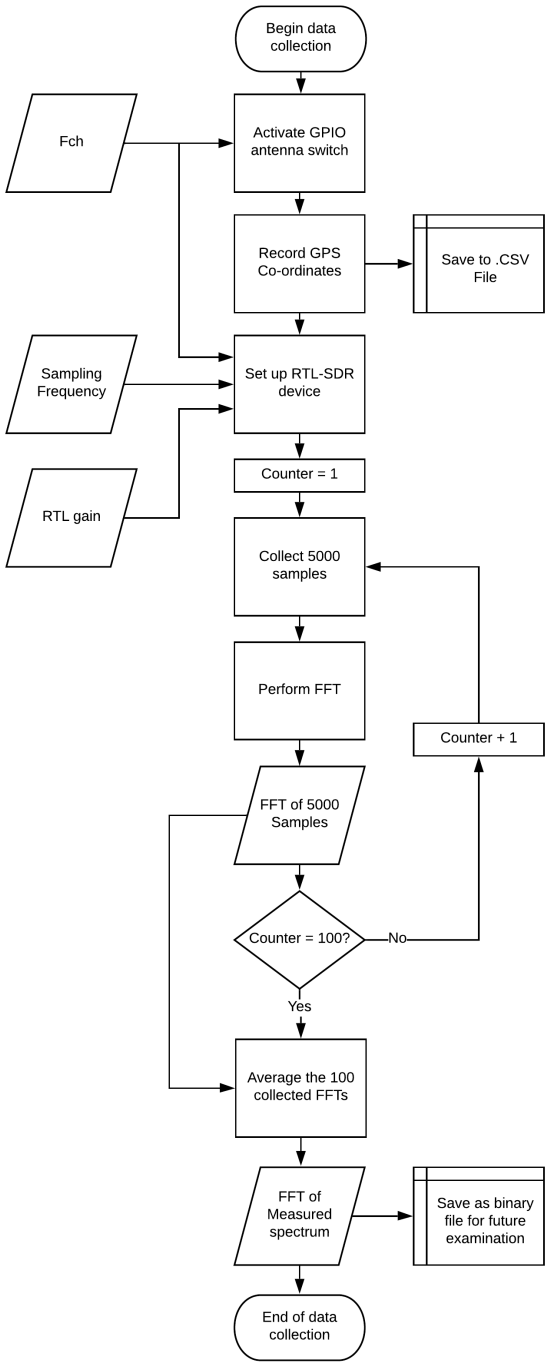

Fig. 4. Description of method of data collection for one frequency

A peak detection routine, which performs a piecewise first order differential on the FFT trace, is run on the FFT in order to identify any peaks within the collected data. The identified peaks are indicated with green dots in Fig. 3.

The detected peaks are searched for a peak within ±50kHz of the current Fch, all peaks outside this ±50kHz area of interest are ignored. These limits are shown as black dotted lines in Fig. 3. If a peak is detected within these boundaries it is recorded, peaks closest to the Fch are recorded first, this is the primary measurement used to determine path loss. If no peak is detected the algorithm instead records the value contained in the FFT bin closest to the current Fch, this is used as a backup primary measurement in the case of a peak detection failure.

A secondary measurement is made of the 3 highest magnitude detected peaks. This measurement is used for later debugging and if a more detailed visual inspection of the spectrum is needed.

An estimation of noise within the FFT is performed by averaging the values in every FFT bin, excluding ones where a peak has been detected. The estimated noise value is shown by the dotted red line in Fig. 3. This estimation will allow an estimated signal-to-noise ratio (SNR) to be calculated later. The peak detection, peak searching and noise estimation are all performed in approximately 1ms.

The information on detected peaks and estimated noise is saved to a .csv file for later post processing. This process takes approximately 16ms.

The entire test involves performing data collection and then initial measurements for an Fch of 71MHz and then repeating the same process for an Fch of 869.525MHz.

The algorithm includes 0.5s pauses while the antennas are being electronically switched. Including the pauses, the entire process is completed for both frequencies in approximately 2.25s. Within the program, measurements for each frequency are recorded within 1.6s of each other.

It is estimated that the instrument will travel at an average walking pace of 1.3m/s. At this speed the maximum Doppler shift that will be expected is 3.8Hz for the 869.525MHz signal. The resolution bandwidth used by the instrument is 409.6Hz, so such a small Doppler shift should be imperceptible [25]. Readings for each frequency are temporally separated by 1.6s, so at a pace of 1.3m/s this means the readings for 71MHz and 869.525MHz will be spatially separated by 2m.

C. Post-processing Calculation Algorithm

Once the data has been collected in the field by the SDR instrument it is then passed for post processing on a PC using MATLAB. The aim of this post processing is to calculate the path loss given by the readings and to produce a model to describe the path loss in the subject environment.

1) Calculating Distance From Recorded GPS Co-ordinates: A method is required to calculate the distance between the TX and each measurement location. The intention of this study is develop a robust instrument that can operate in many different scenarios, in order to increase its usefulness. For short distances, such as the ones in the field test in this paper, a Flat Earth approximation can the used for this calculation. However this approximation will cause a small, unnecessary, error in the results, with the error increasing as larger distances are measured. Changes in latitude of the measurements also create error. Due to the desire to allow a larger study to be completed as part of future work, the Flat Earth approximation will not be used and a more accurate method will be employed.

The Haversine formula was developed by the Royal Navy to allow sailors to calculate the distance between two points on the curved surface of the Earth [26]. In this work the Haversine

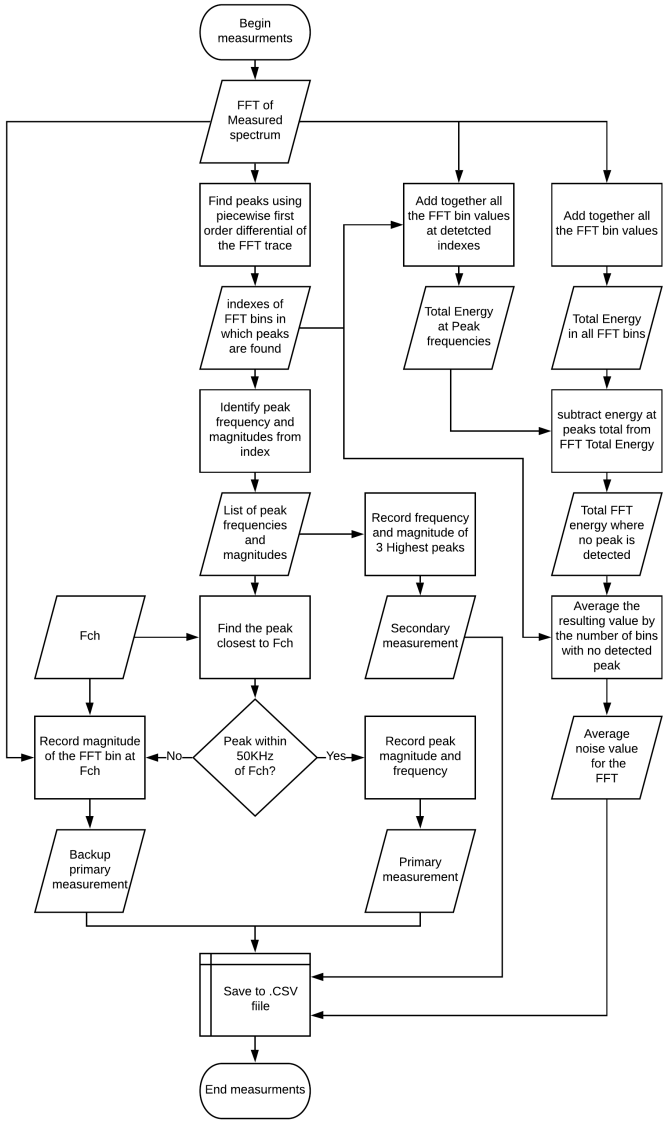

Fig. 5. Description of the method for performing initial measurements for one frequency

formula, as given by (1), will be used to calculate the distance from the TX location to the recorded GPS location of each measurement point.

$$d = 2r\sin^{-1}\left(\sqrt{\sin^2\left(\frac{\varphi_1-\varphi_2}{2}\right)+\cos(\varphi_1)\cos(\varphi_2)\sin^2\left(\frac{\lambda_1-\lambda_2}{2}\right)}\right) \quad (1)$$

where:

d = Distance between 2 points on the surface of Earth (m)
r = Radius of the Earth (m)
$\varphi_1\varphi_2$ = Latitude of point 1 and 2 (radians)
$\lambda_1\lambda_2$ = Longitude of point 1 and 2 (radians)

Point 1 is defined as the TX location which is a known fixed point. Point 2 is given by the GPS co-ordinates recorded with each individual measurement.

2) Calculating Path Loss From Received Power: The path loss at each measurement point is calculated by considering the link budget of the system using (2).

$$P_L = P_{TX} + G_{TX} + G_{RX} - P_{RX} \quad (2)$$

where:

P_L = Path loss (dB)
P_{TX} = Transmission power measured at antenna feed (dBm)
G_{TX} = Transmission antenna gain (dBi)
G_{RX} = Receiving antenna gain (dBi)
P_{RX} = Received power at the calibrated SDR instrument (dBm)

The transmission power is a known value, measured at the antenna feed to eliminate cable losses, which is kept constant throughout the experiment. Received power is provided by the SDR instrument measurements. Gains used for the dipole antennas are 2.15dBi. The helical antenna was measured by the authors and found to have a gain of -14dBi, this is due to it being an electrically small antenna, at only 22cm long and was considered an acceptable compromise in order to produce a portable instrument.

The path loss value given by this equation will include all losses in the environment, including shadowing.

3) Modifying a Log-Distance Model: The path loss of a environment can be described by the log-distance path loss model given in (3) [11]. Received power decays with distance in a log linear fashion, with the path loss exponent controlling the slope of the line. An extra variable can be added to the model to represent shadowing; this is a random variable with a log-normal distribution, the standard deviation of which can be calculated from recorded path loss measurements.

$$P_L(dB) = K + 10\gamma\log_{10}(d) + X_{\sigma dB} \quad (3)$$

where:

$P_L(dB)$ = Path Loss (dB)
K = A constant, depending on antenna characteristics and average channnel attenuation [11]
γ = Path loss exponent
d = Distance between TX and RX (m)
$X_{\sigma dB}$ = log normal random variable with standard deviation of σ (dB)

Values of path loss recorded by the SDR instrument are plotted against the log of the distance between the TX source and the measurement location. Linear regression is used on this data to calculate the path loss exponent γ and constant K, to give a model of the intercept and slope.

4) Calculating Shadowing: Log normal shadowing is a recognised way to model the random variations in received signal strength due to shadowing within an environment [11]. The model, as calculated so far, in the above section will produce a straight line representation of path loss. This straight line is then compared back to the original measurements taken in order to find the standard deviation of these measurements

from the straight line model. Equation (4) [11] shows how this is achieved by comparing the measurement at a specific distance with a prediction from the straight line model at that same distance. The sum of the difference between these two values for every measurement is used to calculate the standard deviation for log normal shadowing.

$$\sigma_{dB} = \sqrt{\frac{1}{n}\sum_{i=1}^{n}[M_{measured}(d_i) - M_{model}(d_i)]^2} \quad (4)$$

where:

σ_{dB} = Standard Deviation (dB)
n = Number of measurements taken
$M_{measured}(d_i)$ = Measured path loss at distance d_i (dB)
$M_{model}(d_i)$ = Predicted path loss at distance d_i (dB)

Together these calculations produce a model which describes the slope of the TX power decay against log distance and the amount of shadowing seen in the area.

D. Measured SDR Instrument Performance

Measurements were taken with the completed SDR instrument in order to assess its performance. The input of the SDR instrument was connected to an Agilent E4437B RF vector signal generator, which was used to output a continuous wave (CW) signal, first at 70MHz and then at 869.525MHz, the power of these signals was increased from -150dBm to 0dBm in 5dBm steps. The gain of the RTL-SDR section of the SDR instrument was also adjusted to several values between the minimum and maximum available values of 0dB and 49.6dB. The output power of the signal generator was compared to the reading produced by the SDR instrument. Readings were also taken with no input provided to the SDR instrument in order to assess the noise floor.

Fig. 6 shows the results for SDR instrument measurements against the signal generator power at 71MHz and Fig. 7 shows the results for 869.525MHz. Gain settings of 0dB (minimum available), 25.4dB, 38.6dB and 49.6dB (maximum available) for the RTL-SDR were used. These figures show that across specific input powers a linear sloping relationship can be seen between the signal generator power and the SDR instrument readings. Within this linear region the instrument can be calibrated to produce accurate readings of received power.

By examining the linear region of each graph, Table II and Table III show the dynamic range and the receive powers covered at each gain setting by the SDR instrument within this region. The displayed average noise level (DANL) at each gain setting is also included. It can be seen that as the gain increases the dynamic range of the SDR instrument decreases, this is due to compression at the upper limit of the RTL-SDR as the noise level increases with gain. The increasing gain also allows lower signal powers to be observed, this is at the cost of being able to observe higher signal powers, due to them saturating the instrument. DANL decreases with increasing gain due to the noise level of the instrument mapping to a lower noise power as the incoming signal is amplified, the higher gain producing a corresponding improvement of the instruments noise figure.

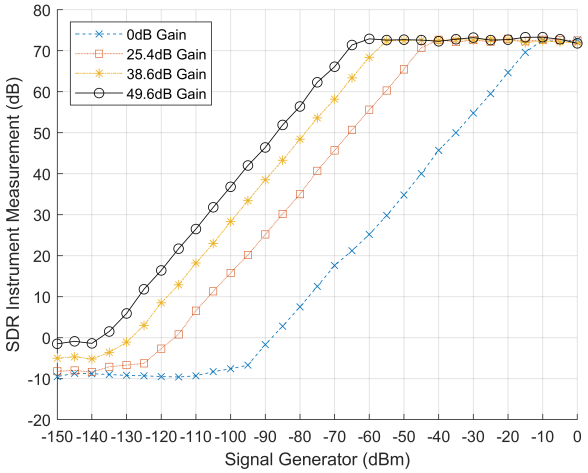

Fig. 6. Readings taken by the SDR instrument using different gain settings at 71MHz when fed a CW signal from a signal generator

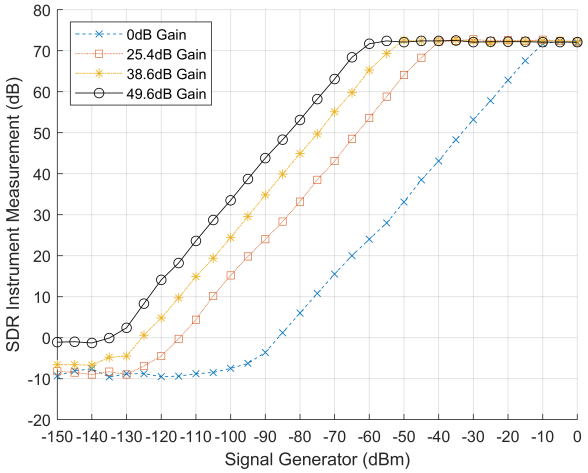

Fig. 7. Readings taken by the SDR instrument using different gain settings at 869.525MHz when fed a CW signal from a signal generator

TABLE II
COMPARISON OF THE PERFORMANCE OF THE SDR INSTRUMENT USING DIFFERENT GAIN SETTINGS AT 71MHZ

Gain (dB)	Dynamic Range (dB)	DANL (dBm/Hz)	RX Power Coverage (dBm)
0	79	-120	-15 to -94
25.4	79	-150	-45 to -124
38.6	78	-159	-55 to -133
49.6	72	-163	-65 to -137

An amplification of 49.6dB was chosen to allow the lowest signal powers to be observed thus giving the instrument higher sensitivity. It is possible to observe a constant difference between the SDR instrument readings and signal generator powers within the linear region, this difference can be used as a calibration offset factor that can be applied to the SDR

TABLE III
COMPARISON OF THE PERFORMANCE OF THE SDR INSTRUMENT USING DIFFERENT GAIN SETTINGS AT 869.525MHZ

Gain (dB)	Dynamic Range (dB)	DANL (dBm/Hz)	RX Power Coverage (dBm)
0	83	-119	-10 to -93
25.4	83	-149	-40 to -123
38.6	80	-156	-50 to -130
49.6	73	-159	-60 to -133

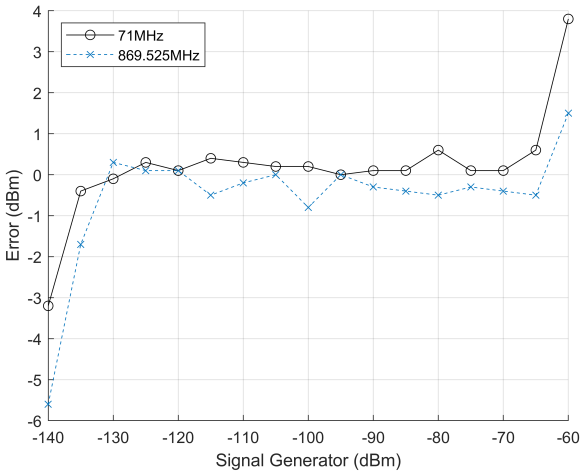

Fig. 8. The error between the signal generator input power and the reading given by the SDR instrument using a gain of 49.6dB at 71MHz and 869.525MHz, after calibration

instrument measurements in order to acquire a reading in dBm. The instrument produces different readings for the same input power at the two different frequencies, this difference is due to the different insertion losses of the RF switch at the different frequencies (1.2dB for 71MHz and 4.8dB for 869.525MHz). This difference necessitates that each of the frequencies be calibrated separately in order to produce an accurate result. The calibration offset factor used for 49.6dB gain is -136.5dB at 71MHz and -133dB at 869.525MHz.

In order to test the calibration of the SDR instrument, signals were fed in to it from the signal generator, the results of this can be seen in Fig. 8. This shows that the SDR instrument is accurate to within $\pm$1dBm across the linear region.

III. FIELD TEST RESULTS

Results are provided for propagation measurements taken by the SDR instrument and a Spectrum Analyzer, these measurements will be compared to assess the accuracy of the SDR instrument.

Fig. 9 shows an urban area of central Sheffield chosen for these measurements, the transmitter is located at co-ordinates 53.380834, -1.478466. Each black dot represents the location of one recorded measurement. As can be seen, multiple measurements were taken on each street to simulate a non-line-of-sight urban IoT deployment. CW signals at both 71MHz and 869.525MHz were broadcast simultaneously with a conducted power of +9.5dBm using dipole antennas.

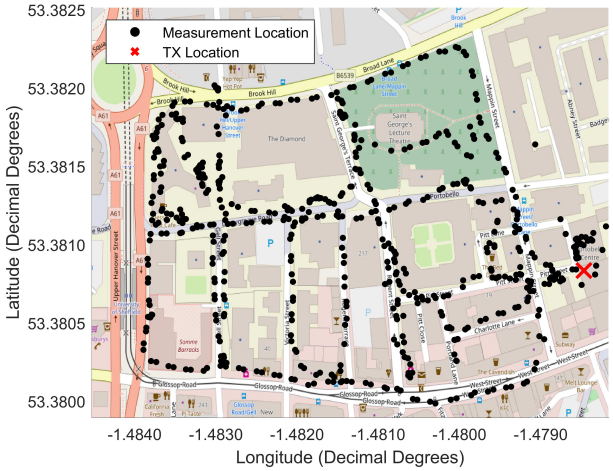

Fig. 9. Map of the test area including GPS locations of each measurement and TX location. Underlying map ©OpenStreetMap contributors www.openstreetmap.org/copyright. [1]

The SDR instrument was carried through the test area with the on-device measurement algorithm running, the test took approximately 1 hour to perform. In total 813 readings were captured by the instrument. Within these readings the 71MHz CW signal was detected 71 times and the 869.525MHz signal was detected 296 times. This gives 71 path loss measurements to calculate the VHF path loss model and 296 measurements to calculate the UHF path loss model. These readings are shown in Fig. 11 and Fig. 12 as cross markers.

Measurements have also been taken with an Anritsu MS2712E portable spectrum analyzer, at a number of locations throughout the test area. Each of these measurements can then be compared to a measurement taken by the SDR instrument at the same location, thus validating the SDR instruments measurements. The spectrum analyzer was set to a RBW of 300Hz, an input attenuation of 0dB and a frequency span of 2MHz in order to match the operation of the SDR instrument as closely as possible. One Antenna was connected to the SDR instrument and the spectrum analyzer at the same time via a splitter to provide both instruments with the same RF signal.

A comparison of one set of measurements taken at the same location by the SDR instrument and the spectrum analyzer is shown in Fig. 10. It can be seen that the readings for both instruments at both frequencies agree to within 0.9dBm.

Table IV shows the absolute differences between SDR instrument and spectrum analyzer readings for all of the measurements taken at the same locations. It can be seen that overall the measurements from each device agreed to a high degree of certainty.

The readings taken be the spectrum analyzer were converted to path loss information, which is shown in Fig. 11 and 12 by the circle markers.

The path loss models created from the SDR instrument readings in Fig. 11 and Fig. 12 are shown in (5) for 71MHz and (6) for 869.525MHz. For 71MHz a path loss exponent (γ) of 2.44 and a shadowing standard deviation (σ) of 8.5dB were calculated. For 869.525MHz a path loss exponent (γ) of

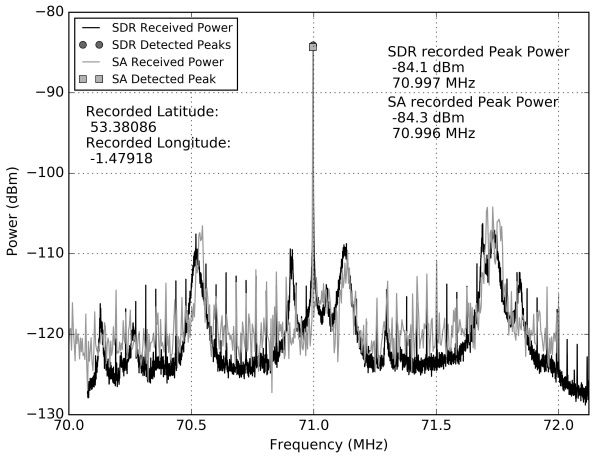

(a) 71MHz signal measurements

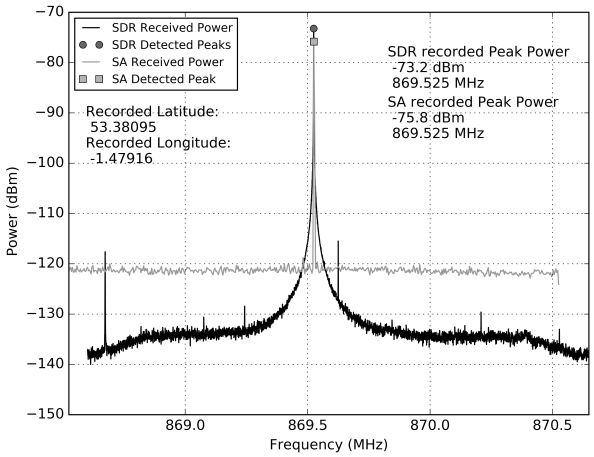

(b) 869.525MHz signal measurements

Fig. 10. A comparison of readings taken by the SDR instrument and the spectrum analyzer at the same location for the same signals

TABLE IV
COMPARISON OF DIFFERENCES BETWEEN READINGS FROM THE SDR INSTRUMENT AND SPECTRUM ANALYZER AT ALL MATCHING LOCATIONS

Frequency (MHz)	Maximum difference (dB)	Average difference (dB)	Standard deviation of average difference (dB)	RMS Difference (dB)
71	4.0	1.3	1.4	1.9
869.525	3.6	1.2	1.1	1.6

4.06 and a shadowing standard deviation (σ) of 8.8dB were calculated.

$$P_{L71}(dB) = 45.3 + 25.6\log_{10}(d) + X_{8.4dB} \quad (5)$$

$$P_{L869}(dB) = 34.1 + 40.6\log_{10}(d) + X_{8.8dB} \quad (6)$$

For the calculation of the shadowing standard deviation part of the Log Distance Model it is assumed that the shadowing follows a log-normal distribution. During the calculation the shadowing present in each measurement is recorded, Fig. 13 shows the cumulative probability distribution of the recorded

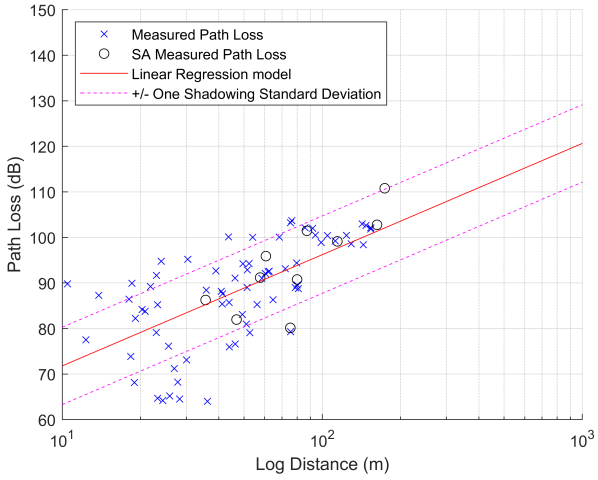

Fig. 11. Measured path loss and the Log Distance Model calculated from the measurements at 71MHz using the SDR instrument, with spectrum analyzer measurements shown for comparison

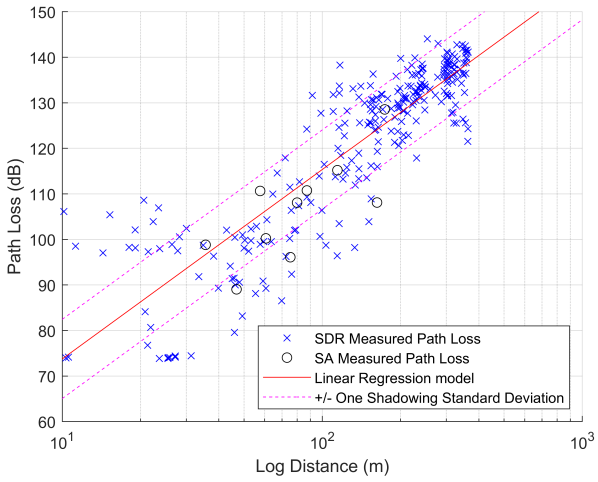

Fig. 12. Measured path loss and the Log Distance Model calculated from the measurements at 869.525MHz using the SDR instrument, with spectrum analyzer measurements shown for comparison

shadowing, confirming that its distribution is indeed log-normal and validating this assumption.

The readings and models developed were compared to the established Hata urban and suburban models given in (7), (8) and (9). These models are commonly used for mobile communication deployments in cluttered environments, however they are only valid for distances over 1km, frequencies of 150MHz to 1500MHz and TX heights above 30m. This means the model is not valid for the use case in this work, but it is included as the closest available widely accepted model found.

$$\begin{aligned} L_{purban} =& 69.55 + 26.16\log_{10}(f_c) - 13.82\log_{10}(h_t) - a(h_r) \\ &+ (44.9 - 6.55log_{10}(h_t))\log_{10}(d) \end{aligned} \quad (7)$$

$$a(h_r) = (1.1\log_{10}(f_c) - 0.7)h_r - (1.56\log_{10}(f_c) - 0.8) \quad (8)$$

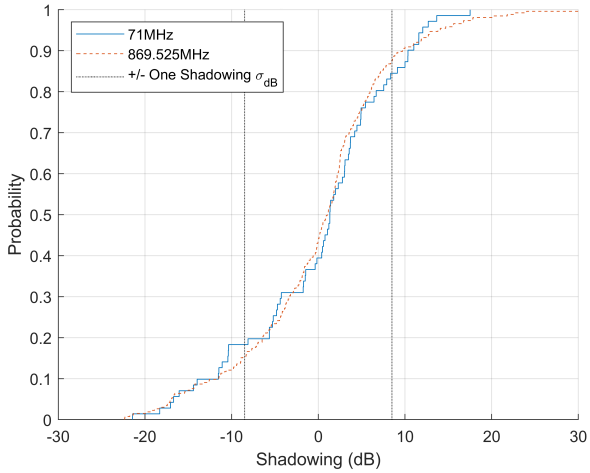

Fig. 13. A cumulative distribution function plot showing the distribution of shadowing measured by the instrument

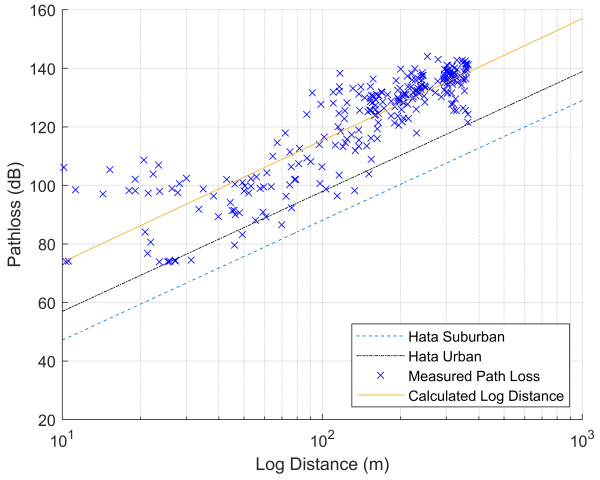

Fig. 15. Measured path loss and the Log Distance Model calculated from the measurements at 869.525MHz,with Hata Urban and Suburban Predictions

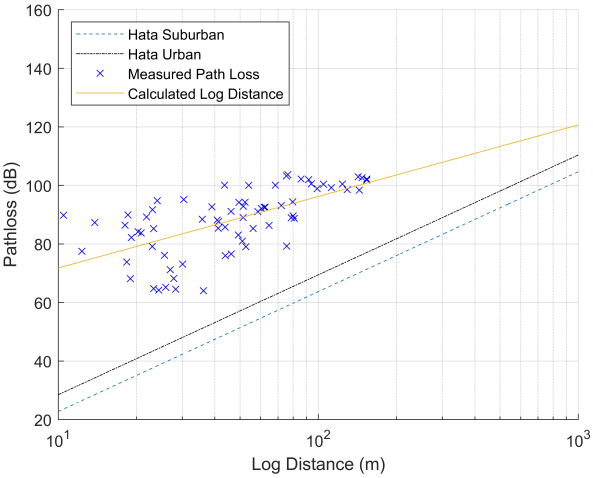

Fig. 14. Measured path loss and the Log Distance Model calculated from the measurements at 71MHz, with Hata Urban and Suburban Predictions

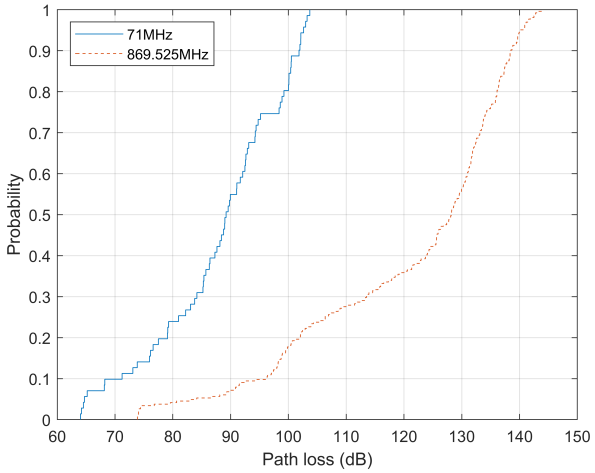

Fig. 16. CDF of measured path loss readings

where:
L_{purban} = Predicted Path loss (dB)
f_c = Frequency (MHz)
h_t = Height of TX antenna (m)
h_r = Height of RX antenna (m)
d = Distance between TX and RX antenna (km)

$$L_{psuburban}(dB) = L_{purban}(dB) - 2\left[\log_{10}\left(\frac{f_c}{28}\right)\right]^2 - 5.4 \quad (9)$$

The measurements taken and model calculated in this work compared to Hata predictions at 71MHz are shown in Fig. 14. It can be seen that the loss measured varies between 40dB and 20dB more than predicted, with slope of the calculated model being less than predicted.

The measurements taken and model calculated in this work compared to Hata predictions at 869.525MHz are shown in Fig. 15. It can be seen that the loss measured is on average 20dB more than predicted, with slope of the calculated model matching the prediction well. It was expected that the Hata models would disagree with the actual measurements due to the models being used outside their specifications. However, it appears that the Hata models are closer to being valid at 896.525MHz than 71MHz.

The cumulative probability function (CDF) of the path loss readings within the test area are shown in Fig. 16. By considering this information and the link budget of a system we can infer the outage probability of a system within the test area. In order to have a maximum outage probability of 10 percent at 71MHz a link budget of at least 102dB is required. At 869.525MHz a link budget of at least 138dB is required.

This shows that signals at 869.525MHz have a much more favorable link budget than at 71MHz. This is unexpected due to VHF usually having more favorable propagation characteristics than UHF, but can be explained by the low gain of the antenna used in the VHF band.

Measurements of detected signal strength, in the order they

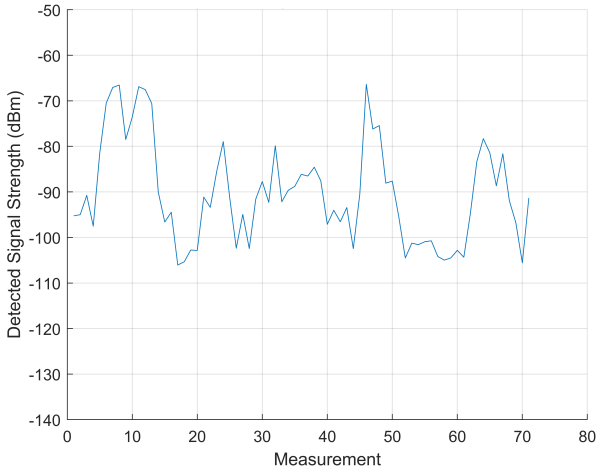

(a) 71MHz Signal Strength for each Measurement

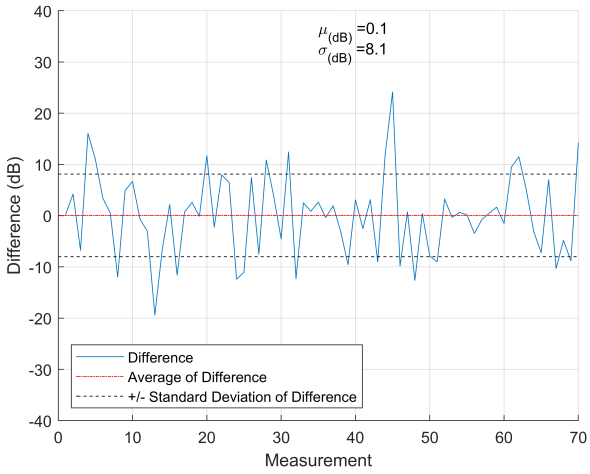

(b) 71MHz Difference Between each Adjacent Signal Strength Measurement

Fig. 17. Readings taken by the SDR instrument in the order they were taken with the difference between each adjacent reading at 71MHz

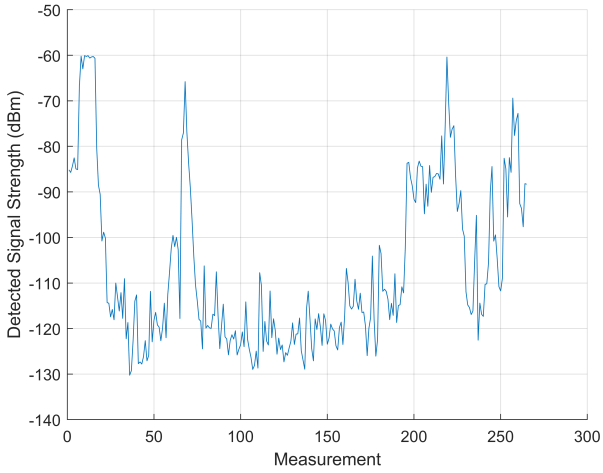

(a) 869.525MHz Signal Strength for each Measurement

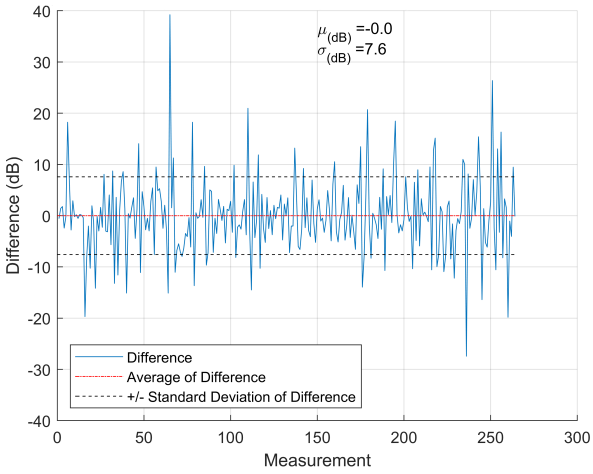

(b) 869.525MHz Difference Between each Adjacent Signal Strength Measurement

Fig. 18. Readings taken by the SDR instrument in the order they were taken with the difference between each adjacent reading at 869.525MHz

were taken, as the instrument was carried through the test area are shown for 71MHz in Fig. 17 and for 869.525MHz in Fig. 18. Because the instrument was carried at 1.3m/s this means that, with the exception of sampling periods where no signal was detected, each measurement for the same frequency is taken 5 seconds apart and is separated by 6.5m. The figures also show the difference between each adjacent measurement.

The average and standard deviation of the adjacent difference are shown in the figures, 71MHz has an average of 0.1dB and a standard deviation of 8.1dB, 869.525MHz has an average of 0.0dB and a standard deviation of 7.6dB. Averages were also taken using the absolute results for adjacent difference so as no to have the negative differences skew the results, it is seen that 6.2dB is the average at 71MHz and 5.3dB is the average at 869.525MHz. These figure include the effect of movement relative to the TX as well as shadowing and multipath effects. Even though no measurement of delay spread was undertaken, the variations shown between the adjacent measurements imply that the readings were taken within a rich channel.

IV. Conclusion

It has been shown that it is possible to perform measurements of the RF spectrum using low cost COTS SDR equipment, to a similar standard as an expensive spectrum analyzer. It has also been shown that hundreds of localized measurements are able to be collected by this instrument in a short space of time, providing extensive data for propagation studies. Due to the inherent ease of re-programming of all SDRs it was possible to develop and deploy new measurement and post-processing algorithms quickly.

The results obtained provide validation of the approach in this work, showing that the results agree with results taken by a commercial spectrum analyzer. It also proves that current models such as Hata do not accurately model propagation within this use case, showing the value of conducting a propagation study with this instrument.

Future work will now be commenced for the use of the developed SDR instrument to perform urban and suburban IoT based propagation studies in a number of different end-

use deployment use-cases in several cities, in order to investigate the possible use of the new VHF spectrum in these environments. The possibility of allowing the instrument to be deployed for measurements using a car will be explored, allowing much larger areas to be covered quickly. The device is currently carried at 1.3m/s and takes 0.24s to collect 5000 samples 100 times, this means that the measurement for an individual frequency is taken over a 0.32m distance, for driving deployments this distance will be longer due to higher speeds. Initial tests on congested city streets at speeds of up to 30km/h (8.3m/s), giving a distance of 1.9m for the measurement, have shown no negative effects on the accuracy of the instrument.

REFERENCES

[1] D. P. Wright and E. A. Ball, "Highly portable software defined radio test bed for dual band propagation studies," in *The Loughborough Antennas Propagation Conference (LAPC 2018)*, Nov 2018, pp. 1–6.

[2] intel, "Guide to iot infographic," September 2017. [Online]. Available: "http://www.intel.com/content/dam/www/public/us/en/images/iot/guide-to-iot-infographic.png"

[3] Sigfox, "Sigfox technology overview," accessed: 13 September 2017. [Online]. Available: "https://www.sigfox.com/en/sigfox-iot-technology-overview"

[4] LoRa Alliance, "What is LoRaWAN?" 2015, accessed: 12 September 2017. [Online]. Available: "https://docs.wixstatic.com/ugd/eccc1a_ed71ea1cd969417493c74e4a13c55685.pdf."

[5] OFCOM, "Vhf radio spectrum for the internet of things," March 2016, accessed: 14 September 2017. [Online]. Available: "https://www.ofcom.org.uk/__data/assets/pdf_file/0029/78563/vhf-iot-statement.pdf"

[6] X. Zhang, T. W. Burress, K. B. Albers, and W. B. Kuhn, "Propagation comparisons at vhf and uhf frequencies," in *2009 IEEE Radio and Wireless Symposium*, Jan 2009, pp. 244–247.

[7] F. Fuschini, M. Barbiroli, G. E. Corazza, V. Degli-Esposti, and F. G., "Analysis of Outdoor-to-Indoor Propagation at 169 MHz for Smart Metering Applications," *IEEE TRANSACTIONS ON ANTENNAS AND PROPAGATION*, vol. 63, no. 4, pp. 1811–1821, 2015.

[8] N. Faruk, O. W. Bello, N. T. Surajudeen-Bakinde, O. Obiyemi, L. A. Olawoyin, M. Ali, and A. Jimoh, "Clutter and terrain effects on path loss in the vhf/uhf bands," *IET Microwaves, Antennas and Propagation*, vol. 12, no. 1, pp. 69–76, 2018.

[9] J. Andrusenko, R. L. Miller, J. A. Abrahamson, N. M. Merheb Emanuelli, R. S. Pattay, and R. M. Shuford, "VHF General Urban Path Loss Model for Short Range Ground-to-Ground Communications," *IEEE TRANSACTIONS ON ANTENNAS AND PROPAGATION*, vol. 56, no. 10, pp. 3302–3310, 2008.

[10] E. A. Ball, "Design and field trial measurement results for a portable and low-cost very-high-frequency/ultra-high-frequency channel sounder platform for internet of things propagation research," *IET Microwaves, Antennas Propagation*, vol. 13, no. 6, pp. 714–724, 2019.

[11] A. Goldsmith, *Wireless Comunications*. Cambridge University Press, 2005.

[12] C. Andrich, A. Ihlow, J. Bauer, N. Beuster, and G. Del Galdo, "High-precision measurement of sine and pulse reference signals using software-defined radio," *IEEE TRANSACTIONS ON INSTRUMENTATION AND MEASUREMENT*, vol. 67, no. 5, pp. 1132–1141, May 2018.

[13] P. Bilski and W. Winiecki, "A low-cost real-time virtual spectrum analyzer," *IEEE TRANSACTIONS ON INSTRUMENTATION AND MEASUREMENT*, vol. 56, no. 6, pp. 2169–2174, 2007.

[14] E. Schmidt, D. Akopian, and D. J. Pack, "Development of a real-time software-defined gps receiver in a labview-based instrumentation environment," *IEEE TRANSACTIONS ON INSTRUMENTATION AND MEASUREMENT*, vol. 67, no. 9, pp. 2082–2096, Sep 2018.

[15] A. Soghoyan, A. Suleiman, and D. Akopian, "A Development and Testing Instrumentation for GPS Software Defined Radio With Fast FPGA Prototyping Support," *IEEE TRANSACTIONS ON INSTRUMENTATION AND MEASUREMENT*, vol. 63, no. 8, pp. 2001–2012, Aug 2014.

[16] S. Yarkan, "A generic measurement setup for implementation and performance evaluation of spectrum sensing techniques: Indoor environments," *IEEE TRANSACTIONS ON INSTRUMENTATION AND MEASUREMENT*, vol. 64, no. 3, pp. 606–614, March 2015.

[17] V. Goverdovsky, D. C. Yates, M. Willerton, C. Papavassiliou, and E. Yeatman, "Modular software-defined radio testbed for rapid prototyping of localization algorithms," *IEEE TRANSACTIONS ON INSTRUMENTATION AND MEASUREMENT*, vol. 65, no. 7, pp. 1577–1584, 2016.

[18] L. Catarinucci, D. De Donno, R. Colella, F. Ricciato, and L. Tarricone, "A Cost-Effective SDR Platform for Performance Characterization of RFID Tags," *IEEE TRANSACTIONS ON INSTRUMENTATION AND MEASUREMENT*, vol. 63, no. 4, pp. 903–911, 2012.

[19] R. Colella, L. Catarinucci, P. Coppola, and L. Tarricone, "Measurement Platform for Electromagnetic Characterization and Performance Evaluation of UHF RFID Tags," *IEEE TRANSACTIONS ON INSTRUMENTATION AND MEASUREMENT*, vol. 65, no. 4, pp. 905–914, April 2016.

[20] C. Stagner, M. Halligan, C. Osterwise, D. G. Beetner, and S. L. Grant, "Locating noncooperative radio receivers using wideband stimulated emissions," *IEEE TRANSACTIONS ON INSTRUMENTATION AND MEASUREMENT*, vol. 62, no. 3, pp. 667–674, March 2013.

[21] S. Majhi, M. Kumar, and W. Xiang, "Implementation and measurement of blind wireless receiver for single carrier systems," *IEEE TRANSACTIONS ON INSTRUMENTATION AND MEASUREMENT*, vol. 66, no. 8, pp. 1965–1975, 2017.

[22] Nooelec, "Nooelec NESDR SMArt SDR - Premium RTL-SDR w/ Aluminum Enclosure, 0.5PPM TCXO, SMA Input. RTL2832U, R820T2-Based," accessed: 06 February 2019. [Online]. Available: "https://www.nooelec.com/store/sdr/nesdr-smart-sdr.html"

[23] RASPBERRY PI FOUNDATION, "Raspberry pi 3 model b," accessed: 31 October 2018. [Online]. Available: "https://www.raspberrypi.org/products/raspberry-pi-3-model-b/"

[24] Y. Liu, "Concurrent dual-band rf signal measurement with adaptive blind feedforward cancellation of wideband receiver nonlinearities," *IEEE TRANSACTIONS ON INSTRUMENTATION AND MEASUREMENT*, vol. 66, no. 8, pp. 1976–1984, Aug 2017.

[25] T. S. Rappaport, *Wireless Communications : principles and practice*. Prentice-Hall, 2002.

[26] Captain, HM Naviation School, *Admiralty Navitagtion Manual, Vol 2*. HM Stationery Office, 1938.

D.P. Wright was born in Wakefield, United Kingdom in 1982. He received the M.Eng degree in electronic engineering from the University of York, York, United Kingdom, in 2013. He is currently studying for the Ph.D degree in electronic engineering from the University of Sheffield, Sheffield, United Kingdom.

From 2014 to 2015 he was with the RAL Space division of Rutherford Appleton Laboratory, Didcot, United Kingdom, focusing on the electronic design of spacecraft instrumentation. His research interests include radio frequency propagation, measurement and software defined radio.

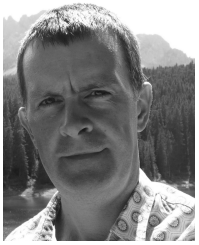

E. A. Ball (M 2008present) Edward (Eddie) became a Member of IEEE in April 2008 and was born in Blackpool, United Kingdom in November 1973. Eddie graduated in 1996 with a 1st Class Master of Engineering Degree in Electronic Systems Engineering, from the University of York, York, United Kingdom.

After graduating, he worked in industry for 20 years, first spending 15 years working as Engineer, Senior RF Engineer and finally Principal RF Engineer at Cambridge Consultants Ltd in Cambridge, UK. He then spent 5 years as Principal RF Engineer and Radio Systems Architect at Tunstall Healthcare Ltd in Whitley, UK. In November 2015 he joined the Department of Electronic and Electrical Engineering at the University of Sheffield, Sheffield, United Kingdom, where he now works as Reader in RF Engineering. His research interests cover all areas of radio technology, from RF system design, RF circuit design (sub-GHz to mm-wave) and the application of radio technology to real-world industrial and commercial problems. He has a particular passion for RF hardware design.

Mr. Ball is a member of the IET and is a Chartered Engineer.